

Lithium intercalation behavior into iron cyanide complex as positive electrode of lithium secondary battery

N. Imanishi ^{a,*}, T. Morikawa ^a, J. Kondo ^a, Y. Takeda ^a, O. Yamamoto ^a, N. Kinugasa ^b,
T. Yamagishi ^b

^a Department of Chemistry, Mie University, 1515 Kamihama-cho, Tsu, Mie 514, Japan

^b Nippon Glass Fiber, 4902 Komori-cho, Takachaya, Tsu, Mie 514, Japan

Received 23 October 1998; accepted 20 January 1999

Abstract

Lithium intercalation of iron cyanide Prussian blue, $\text{Fe}_4[\text{Fe}(\text{CN})_6]_3 \cdot x\text{H}_2\text{O}$, in an aprotic media was examined in regard to the water content inside the lattice. Prussian blue showed reversible lithium intercalation potential around 3 V vs. Li, which corresponds to a redox of iron ions. Two types of water molecules were contained in the structure, one of which called zeolitic water has little effect on lithium intercalation and the theoretical capacity was always observed regardless of its amount. Other coordinating water molecules surrounding Fe^{3+} ions were necessary for the lithium intercalation and their removal by drying beyond 200°C led to a significant capacity decrease. © 1999 Elsevier Science S.A. All rights reserved.

Keywords: Lithium ion battery; Prussian blue; Intercalation; Complex

1. Introduction

There is increasing interests in secondary lithium batteries consisting of intercalation compounds for both the cathode and anode, in accordance with the development of portable electronic equipment, and as a power supply for future electric vehicles and load leveling systems. Lithium ion batteries with the cathodes such as LiCoO_2 , LiNiO_2 , and LiMn_2O_4 can deliver higher energy density compared to the conventional rechargeable batteries [1,2]. LiCoO_2 has been already employed in a practical lithium ion batteries and many efforts to commercialize other two oxides have been made by enhancing the thermal stability in charged state.

In this work, we studied lithium intercalation of transition metal complex and examine the possibility as a new type of positive electrode for lithium secondary battery. Transition metal cyanides, also called cyanometallates, can be recognized as inorganic polymers with a metal cyanide that either combines with another metal cyanide or a free metal cation forming polymeric frameworks [3]. One of the best known examples is an iron cyanide system called

Prussian blue, which was the first chemically prepared material and has been used as a pigment [4]. Prussian blue and its analogues have been studied extensively for their electrochromic behavior and unique magnetic properties [5–10]. It has a three dimensional network consisting of $[\text{Fe}^{2+}(\text{CN})_6]^{4-}$ and Fe^{3+} ions, and an open structure due to the large asymmetric CN^- anion [11]. These open spaces connect each other to form a tunnel structure in the lattice, which can accommodate not only neutral molecules but ions charge-balanced by the iron ions. Prussian blue just prepared is considered to contain water molecules inside this tunnel. According to papers on electrochromic display, topochemical reaction of potassium intercalation into the tunnels show quite high reversibility [12,13].

Through researches in the 1980s, lithium is not considered to intercalate due to the large size of water solvation sphere. However, from aprotic solvent it can be intercalated and owing to low cost of crude materials, easy preparation in liquid phase and controllability of morphology such as fine particle or thin film, Prussian blue is considered a interesting material as the reversible electrode. In this study the attempt to clarify its lithium intercalation mechanism in an aprotic solvent has been made. Because water must be strictly avoided in lithium battery, the role of water molecules which exist inside the

* Corresponding author. Tel.: +81-59-231-9420; Fax: +81-59-231-9478; E-mail: imanishi@chem.mie-u.ac.jp

lattice was mainly discussed in connection to the charge-discharge behaviors.

2. Experimental

Prussian blue samples were prepared by the following method. $\text{FeCl}_3 \cdot 6\text{H}_2\text{O}$ and $\text{K}_4[\text{Fe}(\text{CN})_6]$ were separately dissolved in deoxygenated distilled water then mixed in 4:3 molar ratio at room temperature. Blue-colored precipitate immediately occurred and the suspension was stirred for 3 h to mature. After repeated washing and centrifuging in a diluted HCl solution, it was dried under a nitrogen gas flow at 40°C for 72 h and dried in a temperature range $100\text{--}250^\circ\text{C}$ for 24 h. All the samples were then stored in a sealed glass tube in order not to change the degree of hydration.

Powder X-ray diffraction (XRD) measurements were carried out at the scanning speed of $0.5^\circ \text{min}^{-1}$ by a Rigaku Rotaflex diffractometer with Cu $\text{K}\alpha$ radiation at 40 kV, 150 mA. During the measurements samples were kept in an argon atmosphere to avoid moisture. Water content was determined from thermogravimetric analysis and the Karl–Fischer titration technique.

A button cell was used to measure the electrochemical properties of the material. It has an identical dimension to a commercial CR2025 cell, of which the upper and lower sides are 20 mm in diameter and the total thickness is 2.5 mm. The cathodes were prepared by mixing Prussian blue powder with acetylene-black conductive agent (20 wt.%), and polytetrafluoroethylene binder (0.1 wt.%) which were dried before use. The mixture was pressed into a disc-shape and put on a stainless steel mesh working as a current collector. Consequently, the cathode electrode having about 1 mm thickness was obtained. A lithium metal sheet was used as the anode and put on the counter side of the cell. A nonwoven fabric of polypropylene was used as a separator soaked with one molar solution of LiClO_4 in a propylene carbonate/1,2-dimethoxy ethane mixture. The cell was assembled in a dry argon filled glove box. The charge-discharge cycling tests of these cells were carried out at a constant current density of 0.1 mA cm^{-2} between 1.6 and 4.3 V cut-off voltages. These voltages were set because the electrolyte begins to decompose above 4.3 V and the irreversible reaction due to the Prussian blue is observed below 1.6 V.

3. Results and discussions

Two stoichiometries, the $\text{KFeFe}(\text{CN})_6$ so-called soluble form and the $\text{Fe}_4[\text{Fe}(\text{CN})_6]_3$ so-called insoluble form, are proposed for Prussian blue. The analytical data demonstrate that our sample has a composition close to that of the ideal insoluble form. Using thermogravimetric analysis, as-prepared sample which was dried in air at 40°C for

1 week has about 14 water molecules per unit formula. This composition is consistent with the work on a single crystal done by Buser et al. [14] in which the chemical formula was described as $\text{Fe}_4^{3+}[\text{Fe}^{2+}(\text{CN}^-)_6]_3 \cdot 15\text{H}_2\text{O}$. Here, Fe^{3+} coordinated by an N atom is in the d^5 high spin state, while Fe^{2+} coordinated by a C atom is in the d^6 low spin state. The 14 water molecules are considered to be mainly located in the lattice and if any small amount of surface water exists.

Fig. 1 shows a crystal structure of the insoluble form reported in literature [14]. From the mole ratio of Fe^{3+} and $\text{Fe}(\text{CN})_6^{4-}$, 1/4 of Fe^{2+} sites are unoccupied, leading to statistically distributed vacancies if assuming a face-centered unit cell. The figure describes a completely ordered structure, in which the vacancy is located at the center of the unit cell. A real product is considered to have various crystallinities between these two extreme structures depending on the preparation procedures. Our sample was precipitated in quite a short time so that highly disordered vacancies can be expected. Fe^{3+} ions next to vacancies have a chemically coordinating water molecule whose total number in the unit is six, and another kind of water molecule weakly adsorbs internal open space of the unit cell. The drying process reduces the number of these water molecules in order of surface adsorbed, physically adsorbed zeolitic, and chemically coordinating ones. Fig. 2 shows a measured XRD pattern of the as-prepared Prussian blue sample. The pattern reveals that the sample can be indexed by $Fm3m$ symmetry and contains no impurity phase. Regarding the broad diffraction pattern that is far from a highly crystalline structure, and lack of reflections due to ordering, the random distribution of the Fe^{2+} vacancy seems appropriate.

To understand the hydration behavior of Prussian blue, thermogravimetry (TG)-differential thermal analysis (DTA) was performed from room temperature to 900°C at a heating speed of 3°C min^{-1} . A typical TG-DTA curve recorded in an air atmosphere is presented in Fig. 3. From

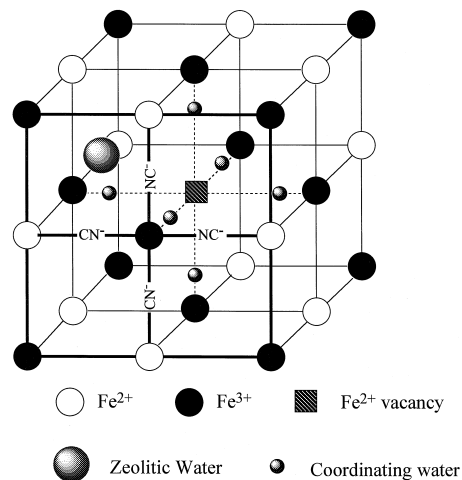


Fig. 1. The ideal crystal structure of insoluble Prussian blue.

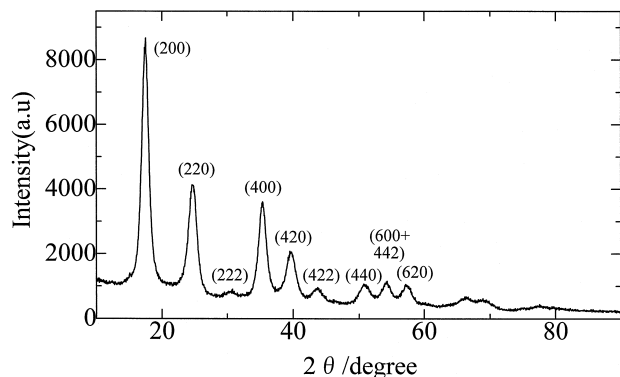


Fig. 2. The typical powder X-ray diffraction pattern of as-prepared Prussian blue.

room temperature to 200°C, the smooth decreasing TG curve and a broad endothermic DTA peak shows the process of dehydration from the surface and deintercalation of the zeolitic water. A TG plateau appearing around 200°C indicates a stable phase with a specific number of water molecules. Beyond 200°C there is an abrupt weight decrease and a simultaneous sharp exothermic DTA peak demonstrates the oxidation of Prussian blue by air. Even in an inert atmosphere such as nitrogen, a much smaller but distinct weight loss was observed possibly due to a reaction with oxygen from the coordinating water molecules. The final product after heating up to 900°C was confirmed as α -Fe₂O₃ by XRD measurement. By taking the weight difference between two plateaus at 200 and 900°C into consideration, the stable phase composition at 200°C was calculated as Fe₄[Fe(CN)₆]₃ · 5.89H₂O. The similar calculation result was obtained for samples with different degrees of hydration. From the structure model shown in Fig. 1, it is rational to consider that these six water molecules are coordinating type and the zeolitic and surface adsorbed water coexist only below this temperature. It is notable that the last six water molecules can not be removed by heating without a lattice collapse. Consequently the five heating temperatures, 40, 100, 150, 200, and 250°C, were chosen in order to understand the effect of the amount of water

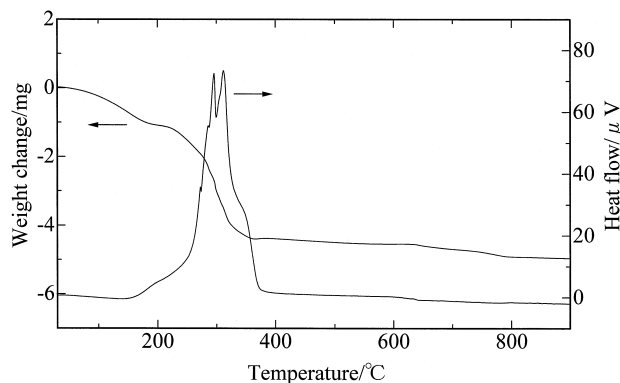


Fig. 3. Thermogravimetric and differential thermal analysis curves scanned from room temperature to 900°C.

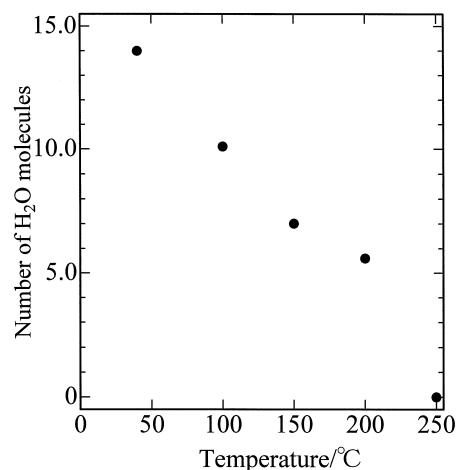


Fig. 4. The number of water molecules contained per unit cell in samples heat treated at various temperatures.

molecules on the lithium intercalation behavior. The hydration numbers calculated from the analysis against these heating temperatures are summarized in Fig. 4.

XRD patterns of Prussian blue heated at the five different temperatures do not show large changes in the position and intensity as shown in Fig. 5. The loss of zeolitic water by drying up to 200°C was not clearly reflected in the relative peak intensities in the XRD patterns. Only the sample dried at 250°C shows several diffraction peaks marked by a closed circle belonging to an unknown second phase, which is considered to result from the lattice decomposition shown in the thermal analysis.

The relation between the fcc lattice parameter and experimentally determined hydration number is plotted in Fig. 6. It initially shows a slight increase with losing water, then drastically increases when the number goes below six. The first small expansion is caused by loss of zeolitic water molecules. The six coordinating water molecules around Fe³⁺ ions are more tightly bound to the lattice by chemical forces and start leaving after all the zeolitic water is dried away. The steep lattice expansion at high temperatures can be explained by this loss of the coordinating

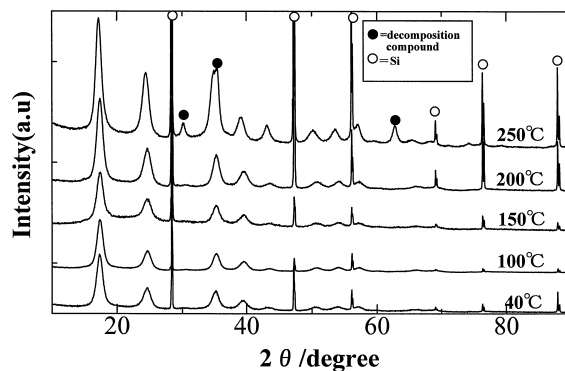


Fig. 5. The X-ray diffraction patterns of samples heat treated at various temperatures.

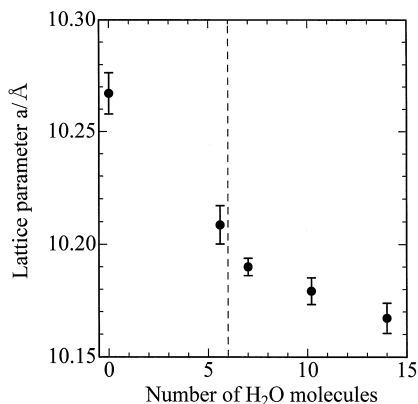


Fig. 6. The lattice parameter changes of Prussian blue fcc unit cell against the degrees of hydration.

water molecules. Fe^{3+} with no ligands are expected to induce a strong electrostatic repulsion with surrounding ions leading to a highly expanding lattice.

The electrochemical behaviors of Prussian blue samples dried at various temperatures are shown in Fig. 7. All the curves show the first, second and tenth discharges and following charge profiles. The result of the sample heated at 150°C was quite similar to that of the sample heated at 100°C. The initial open circuit potentials of the cells were 3.5 V for samples heated at 40 and 100°C, and 3.2 V for ones heated at 200 and 250°C. The average charge–discharge potential of the Prussian blues are about 3 V regardless of the hydration degrees. This is consistent with

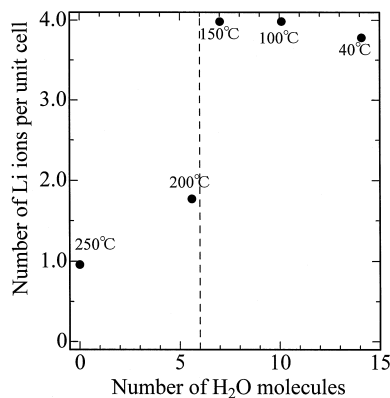


Fig. 8. The intercalated lithium number per unit cell as a function of the hydration number.

the reported potential of 0.2 V vs. SCE in aqueous electrolytes along with cation intercalation. The typical S-shaped profile indicates a single phase lithium intercalation onto one specific site.

The comparison among these four samples leads to consideration that the capacity of Prussian blue strongly and nonlinearly depends on the water content. It gradually increases with increasing drying temperature up to 150°C, then a significant decrease to 40 mA h g⁻¹ for the sample dried at 250°C is observed. The highest discharge capacity of about 110 mA h g⁻¹ was observed in the case of the samples dried at 100 and 150°C. The theoretical capacities of the former, $\text{Fe}_4[\text{Fe}(\text{CN})_6]_3 \cdot 10\text{H}_2\text{O}$, and the latter,

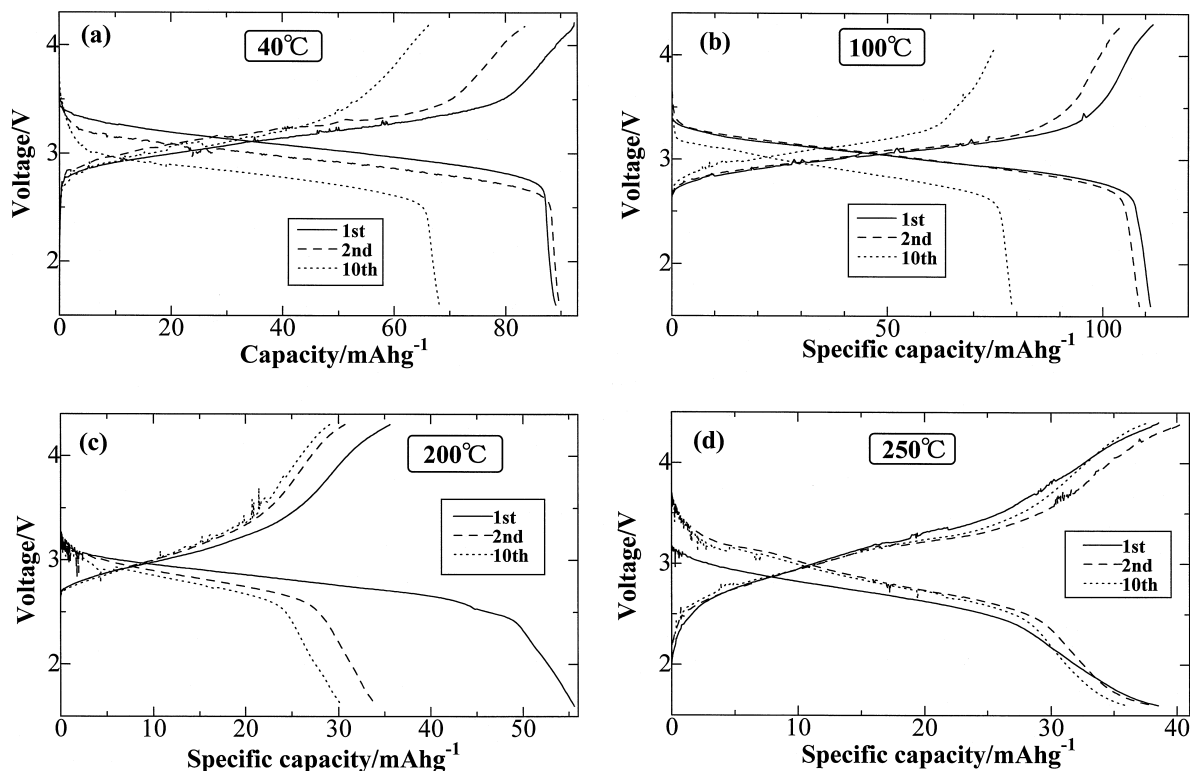


Fig. 7. Charge–discharge curves of Prussian blue heated at (a) 40°C, (b) 100°C, (c) 200°C, and (d) 250°C.

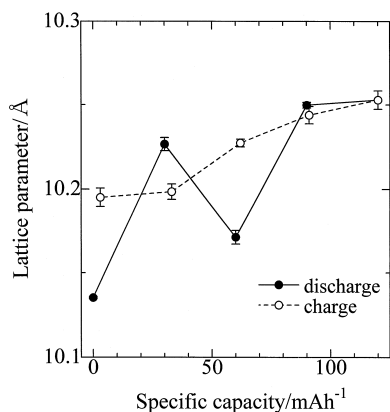
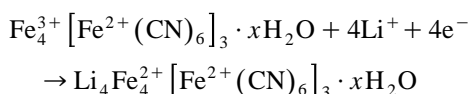


Fig. 9. The lattice parameter changes along with the first discharge and charge of the sample heated at 100°C.

$\text{Fe}_4[\text{Fe}(\text{CN})_6]_3 \cdot 7\text{H}_2\text{O}$ is 103 and 109 mA h g^{-1} , respectively, assuming that one unit cell accommodates four lithium ions as the following reaction.



These values and observed data coincide within an experimental error, which demonstrates that a full discharge state was always achieved. The normalized capacity described as the number of lithium per unit cell is shown in Fig. 8. The samples dried at 40, 100 and 150°C have the maximum four accommodated lithium ions at the end of discharging, although they have different numbers of water molecules. No relation of the polarization behaviors against the hydration degree reveals that existence of the zeolitic water does not influence the lithium intercalation process.

The samples dried at 200 and 250°C show significantly smaller accommodation numbers of lithium than samples dried below 200°C. The difference between these two groups is the number of coordinating water molecules. The small capacity, therefore, can be attributed to the lack of coordinating water molecules. To conclude, they have an important role in order to accommodate and transport lithium to the neighboring sites.

The poor cyclability such as 30% capacity fading through 10 cycles is commonly observed and is a serious problem as an electrode for a rechargeable battery. Therefore, the structural change during the first cycle was examined by XRD. All the discharged or charged samples were kept rest for 48 h to equilibrate before measurements. The lattice parameters of the samples with various lithium content are shown in Fig. 9. The irregular but reproducible change in discharge process can not be rationalized at this stage of the study. The inconsistency between the profiles of intercalation and deintercalation indicates that topochemical reaction does not occur in this material.

However, in the XRD patterns there are no signs of phase transitions nor structure degradations. So we consider that the water content changes by lithium intercalation. Further insight of the structure such as lithium site determination by neutron diffraction, etc., is necessary to explain this irregular change and reveal the cause of the irreversibility.

4. Conclusions

Prussian blue as a positive electrode for a lithium rechargeable battery can deliver a 110 mA h g^{-1} maximum capacity at a discharge potential of 3.0 V. The electrochemical behavior strongly depends on the number of coordinating water molecules, although the zeolitic ones have little effect. The samples with 6–10 water molecules show the highest charge–discharge capacity. The present performance is far from satisfactory level from a practical point of view. This is mainly because the 3/7 of the transition metal in the matrix cannot be available in the redox process. This problem can be solved by applying a complex consisting of two kind of metals both having a 3+ valence state. If a complex, $\text{A}^{3+} [\text{B}^{3+} (\text{CN})_6]$ ($\text{A} = \text{V}, \text{Cr}, \text{Fe}; \text{B} = \text{Mn}, \text{Fe}, \text{Co}$), can be synthesized, two lithium can be accommodated resulting in about 200 mA h g^{-1} of theoretical capacity. Another advantageous point of this formula is no cation vacancy in the framework, which leads to no coordinating water molecules and provides more suitable situation for lithium battery.

References

- [1] L. Guohua, H. Ikuta, T. Uchida, M. Wakihara, *J. Electrochem. Soc.* 143 (1996) 178.
- [2] C. Delmas, I. Saadoun, *Solid State Ionics* 53–56 (1992) 370.
- [3] T. Iwamoto, *J. Inclusion Phen. Mol. Recognition Chem.* 24 (1996) 61.
- [4] Anonymous, *Miscellanea Berolinensia ad Incrementum Scientiarum*, Vol. 1, Berlin, 1710, p. 377.
- [5] K.P. Rajan, V.D. Neff, *J. Phys. Chem.* 86 (1982) 4361.
- [6] D. Ellis, M. Eckhoff, V.D. Neff, *J. Phys. Chem.* 85 (1981) 1225.
- [7] J.P. Ziegler, B.M. Howard, *Solar Energy Materials and Solar Cells* 39 (1995) 317.
- [8] S. Ferlay, T. Mallah, R. Ouahes, P. Veillet, M. Verdager, *Nature* 378 (1995) 701.
- [9] W.R. Entley, C.R. Treadway, G.S. Girolami, *Mol. Cryst. Liq. Cryst.* 273 (1995) 153.
- [10] O. Sato, Y. Einaga, T. Iyoda, A. Fujishima, K. Hashimoto, *J. Electrochem. Soc.* 144 (1997) L11.
- [11] J.F. Keggin, F.D. Miles, *Nature* 137 (1936) 577.
- [12] K. Itaya, T. Ataka, S. Toshima, *J. Am. Chem. Soc.* 104 (1982) 4767.
- [13] K. Itaya, H. Akahoshi, S. Toshima, *J. Electrochem. Soc.* 129 (1982) 1498.
- [14] H.J. Buser, D. Schwarzenbach, W. Petter, A. Ludi, *Inorg. Chem.* 16 (1977) 2704.